



## Research Article

# Life Cycle Assessment of CO<sub>2</sub>-to-methanol: Comparative Evaluation of Direct and Alcohol-Assisted Hydrogenation Routes

Chayet Worathitanon<sup>1</sup>, Naphat Chansonthi<sup>1</sup>, Pawat Pinthong<sup>1</sup>, Kritsana Suwanamad<sup>2</sup>,  
Viganda Varabuntoonvit<sup>1,3,\*</sup>

<sup>1</sup> Department of Chemical Engineering, Faculty of Engineering, Kasetsart University, Bangkok 10900, Thailand

<sup>2</sup> Department of Chemical Engineering, Faculty of Engineering, Chulalongkorn University, Bangkok 10330, Thailand

<sup>3</sup> The Center of Excellence on Petrochemical and Materials Technology, Chulalongkorn University, Bangkok 10330, Thailand

\*Corresponding Email: fengvgv@ku.th

## Abstract

The increasing severity of global warming, which is driven primarily by greenhouse gas emissions, underscores the urgent need for CO<sub>2</sub> reduction and utilization strategies. Converting CO<sub>2</sub> into methanol is a promising approach, as methanol serves both as a fuel and a feedstock in various industries. This study evaluated the life cycle environmental impacts of three methanol production routes: (1) direct CO<sub>2</sub> hydrogenation, (2) ethanol-assisted CO<sub>2</sub> hydrogenation, and (3) propanol-assisted CO<sub>2</sub> hydrogenation. Two energy scenarios are considered: conventional energy and wind power. Process simulations were performed via Aspen Plus V.14, and inventories were analyzed through Life Cycle Assessment (LCA) via the ReCiPe 2016 (H) method under a cradle-to-gate approach for 1,000 kg of methanol. The alcohol-assisted processes operated at a lower reaction temperature (150 °C) and consumed less CO<sub>2</sub>, H<sub>2</sub>, and compression energy than did the conventional process (250 °C), thereby reducing the environmental impact. However, methanol purification remains energy intensive. Under conventional energy, the propanol-assisted process presented the highest global warming potential (GWP), followed by the ethanol-assisted process, whereas the conventional route presented the lowest GWP. The elevated impact of the propanol route was attributed primarily to increased alcohol feedstock and energy consumption. The use of wind power significantly reduced the GWP in the separation stage of alcohol-assisted routes, resulting in the lowest GWP for the ethanol-assisted process.

## ARTICLE HISTORY

Received: 25 Jul. 2025

Revised: 25 Oct. 2025

Accepted: 19 Dec. 2025

Published: 23 Dec. 2025

## KEYWORDS

Life cycle assessment;  
CO<sub>2</sub> hydrogenation;  
Alcohol-assisted CO<sub>2</sub>  
hydrogenation;  
Methanol production;  
Carbon utilization

## Introduction

CO<sub>2</sub> emissions from human activities continue to rise, reaching approximately 37.8 Gt in 2024, and drive the global climate crisis, as evidenced by rising temperatures, more intense extreme weather events, melting glaciers, and ocean acidification (Bolan et al., 2024; International Energy Agency, 2025). In response, carbon capture and storage (CCS) and carbon capture and utilization (CCU) have emerged as key technologies for reducing emissions. According to a 2024 literature review, 51 operational CCS facilities currently capture

approximately 50 million tonnes of CO<sub>2</sub> annually (El Farsaoui et al., 2025). Compared with global emissions, this capacity highlights a substantial gap, emphasizing the urgent need for CCU technologies that convert CO<sub>2</sub> into valuable products.

Methanol is one of the most extensively studied CO<sub>2</sub>-derived products because of its widespread industrial applications and its role as an intermediate in the production of formaldehyde, acetic acid, and olefins. Methanol production methods include natural gas reforming, CO<sub>2</sub> hydrogenation, and gasification. However, reforming

and gasification result in significant CO<sub>2</sub> emissions because they rely on carbon-intensive feedstocks and require high operating temperatures—700–1,000 °C for reforming and 900–1,400 °C for gasification (Ahmed et al., 2019; Dinca et al., 2018; Mohamed et al., 2021). In contrast, direct hydrogenation provides a more sustainable pathway because of its lower operating temperature (200–300 °C) and direct utilization of CO<sub>2</sub> (Kim et al., 2022). Nevertheless, this route faces technical challenges: it is highly exothermic, achieves low CO<sub>2</sub> conversion rates, and yields limited methanol. For example, when a commercial Cu/ZnO/Al<sub>2</sub>O<sub>3</sub> catalyst is used, the CO<sub>2</sub> conversion reaches only 23% at 300 °C and 1 MPa, with a methanol yield of only 0.06% at 300 °C and 0.1 MPa (Yusuf and Almomani, 2023).

To address the limitations of direct CO<sub>2</sub> hydrogenation, the alcohol-assisted method has been developed to increase the methanol yield by improving CO<sub>2</sub> solubility and activation, thereby increasing its local concentration at the catalyst surface (Ye et al., 2023). Lighter alcohols, such as ethanol, generally promote higher conversion rates and fewer side reactions than heavier alcohols do, although ethanol–methanol azeotrope formation can complicate downstream separation (Esfahani et al., 2023; Likhittaphon et al., 2019). In contrast, heavier alcohols such as propanol reduce azeotrope-related separation issues but result in greater formation of acetate byproducts (Likhittaphon et al., 2019). Additionally, alcohols enhance catalyst activity by stabilizing active sites, improving metal dispersion, and lowering the energy barrier, which allows for milder reaction conditions (150 °C), suppresses side reactions such as reverse water–gas shift and methane formation, and leads to higher methanol selectivity and overall process efficiency (Zeng et al., 2002).

To evaluate environmental performance, a life cycle assessment (LCA) is conducted in accordance with ISO standards. While LCA studies on direct hydrogenation are relatively comprehensive, comparative assessments with alcohol-assisted routes remain limited. The existing data are primarily gate-to-gate; one study reported annual CO<sub>2</sub> emissions of approximately 30,000 t for the ethanol-assisted route versus 10,000 t for direct hydrogenation, largely due to the energy-intensive distillation required for alcohol recovery and recycling. This underscores the need for a complete cradle-to-gate LCA of the alcohol-assisted process (Mungchan, 2021).

With improvements in technology and energy efficiency, electricity from onshore wind power now presents a highly promising alternative to conventional sources. Wind energy offers a low life cycle carbon intensity of approximately 20.37 g CO<sub>2</sub> equivalent per kWh over a 20–25-year operational lifespan (Xu et al., 2022). It also causes minimal harm to water quality and human health, with significantly lower toxicity levels

than fossil fuel-based power sources (Saidur et al., 2011). These environmental advantages make wind energy a critical enabler of sustainable development and emission reduction. This study therefore conducts a cradle-to-gate LCA to compare methanol production via direct hydrogenation and alcohol-assisted routes using ethanol and propanol. The objective is to clarify the differences in the environmental impacts and energy consumption across the three production routes under both conventional and wind-based energy scenarios.

## Materials and methods

### 1) Process simulation

Aspen Plus V.14 was used to develop simulation models for comparing methanol production via direct hydrogenation and alcohol-assisted routes on the basis of the methodology adapted from Mungchan (2021). The predictive Soave–Redlich–Kwong (PSRK) thermodynamic model was selected for its suitability for handling gases and polar compounds under high-pressure conditions above 10 bar. To maintain a consistent basis for evaluating environmental impacts, the methanol production rate was fixed at 1,000 kg h<sup>-1</sup>. The analysis included three cases: direct hydrogenation, an alcohol-assisted process using ethanol, and an alcohol-assisted process using propanol. The uncertainty in the Aspen Plus simulation was reduced in both the mass and energy balances by verifying the chosen thermodynamic model and cross-checking the results against data from previous experimental and simulation studies performed under comparable operating conditions [Mungchan, 2021; Van-Dal and Bouallou, 2013].

#### 1.1) Direct hydrogenation (Case 1)

In Case 1, methanol production via direct CO<sub>2</sub> hydrogenation under isothermal conditions was simulated via the reaction kinetics proposed by Van-Dal et al. [16] (Figure 1). CO<sub>2</sub> and H<sub>2</sub> were individually compressed to 5 MPa through three-stage compressors with intercooling and then mixed with the recycle stream at a molar ratio of 1:3 (CO<sub>2</sub>:H<sub>2</sub>). The combined stream was heated to 523 K before it entered the reactor. After the reaction, the product stream was cooled to 349 K and directed to a flash drum for gas–liquid separation. Unreacted gases in the vapor phase were recycled, whereas the liquid phase underwent further separation in a second flash vessel. A 23-tray distillation column separated methanol and water, producing high-purity methanol at the top and removing water at the bottom.

#### 1.2) Alcohol-assisted process using ethanol (Case 2)

In Case 2, ethanol was used as a catalytic solvent in the alcohol-assisted methanol synthesis route (Figure 2). A feed ratio of CO<sub>2</sub>:H<sub>2</sub>:ethanol of 1:3:1 was applied. Ethanol was pressurized to 5 MPa and blended with a recycled stream from the solvent recovery column.

The reactor was operated at 423 K and 5 MPa. Following the reaction, the product stream was cooled and sent to a flash vessel for phase separation. Unreacted gases were recycled to the reactor. The resulting liquid mixture of methanol, ethanol, and water was introduced into a 9-tray distillation column, which separated the methanol and residual gas at the top and retained the methanol–ethanol–water mixture at the bottom. A second 53-tray column further refined methanol by removing ethanol and water, while a 10-tray column recovered ethanol for reuse.

### 1.3) Alcohol-assisted process using propanol (Case 3)

Case 3 modeled the alcohol-assisted methanol synthesis process using n-propanol as a catalytic solvent. The feed conditions and molar ratios were identical to those in Case 2. The reactor was operated at 423 K and 5 MPa. After the reaction, the product stream was cooled and directed to a flash vessel for gas–liquid separation. Unreacted gases were recycled to the reactor. The bottom stream, which is primarily composed of methanol, n-propanol, water, and propyl propionate, was sent to a 27-tray atmospheric distillation column. Methanol and water were collected at the top, while n-propanol and propyl propionate were removed at the bottom. A second 21-tray column further purified

methanol by separating residual water. A 19-tray solvent recovery column was used to reclaim n-propanol for recycling.

## 2) Life cycle assessment

This study aimed to evaluate the environmental performance of alcohol-assisted methanol synthesis compared with that of conventional direct CO<sub>2</sub> hydrogenation. The LCA was conducted via SimaPro V.10.2, applying the ReCiPe 2016 (Hierarchist) method to assess midpoint impacts and perform normalization. The ReCiPe methodology was selected because of its widespread adoption in LCIA studies and its ability to assess multiple impact categories, including climate change, human health, and ecosystem quality. The hierarchist (H) perspective was used, as it is the most commonly applied and is based on scientific consensus for medium-term effects (Schumacher, 2016). A functional unit of 1,000 kg of methanol was established for consistent comparison. The assessment followed a cradle-to-gate approach. Inventory data for methanol production were derived from process simulations in Aspen Plus V.14, whereas raw material and energy acquisition data were obtained from the Ecoinvent 3.10 database. The system boundaries for each case are shown in Figure 4.

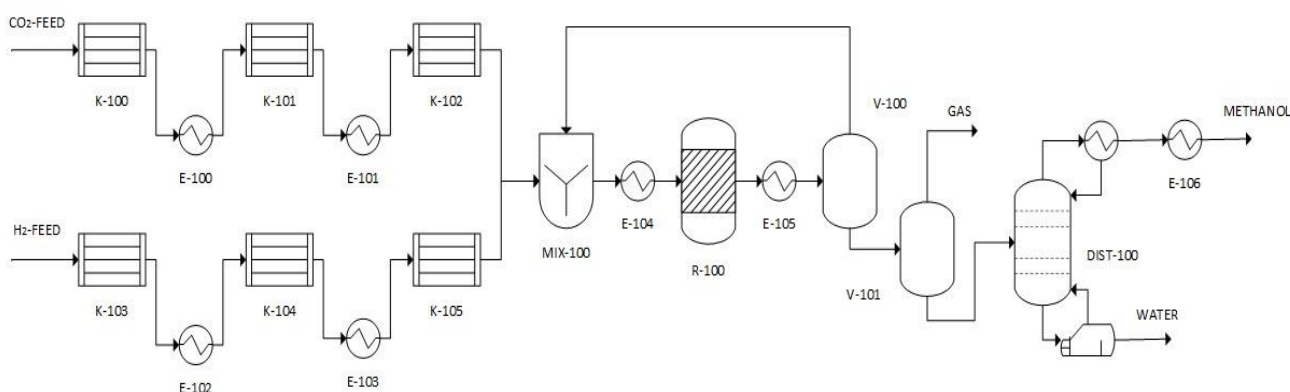


**Figure 1** Process flow diagram of direct hydrogenation for methanol production.

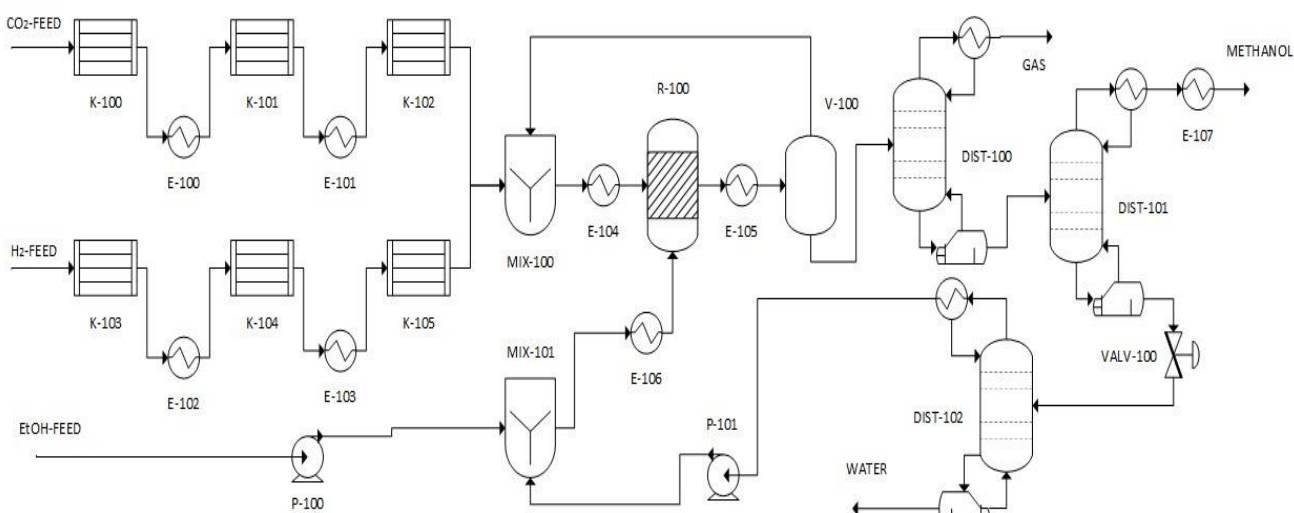


**Figure 2** Process flow diagram of alcohol-assisted hydrogenation using ethanol for methanol production.

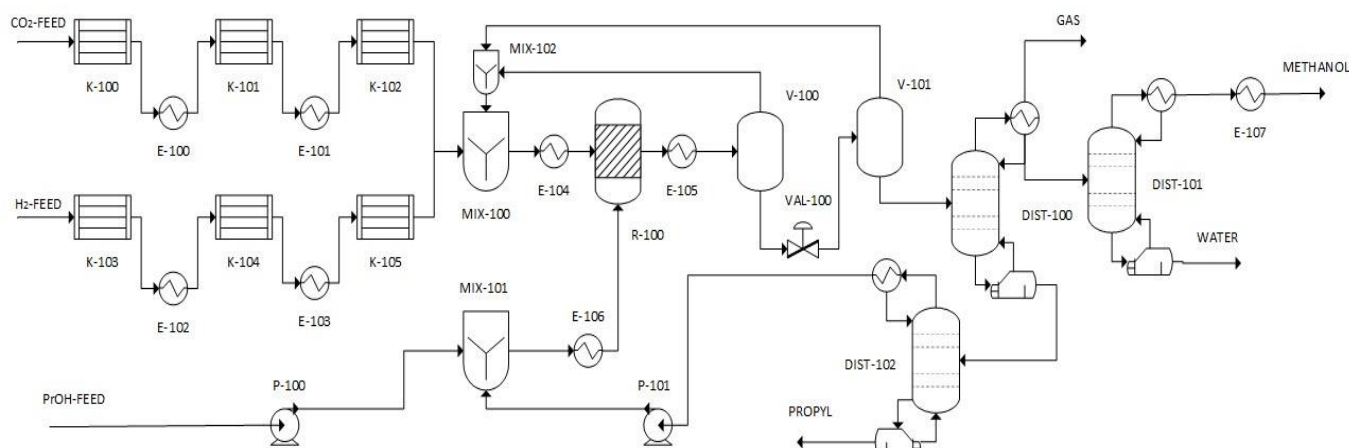


**Figure 3** Process flow diagram of alcohol-assisted hydrogenation using propanol for methanol production.

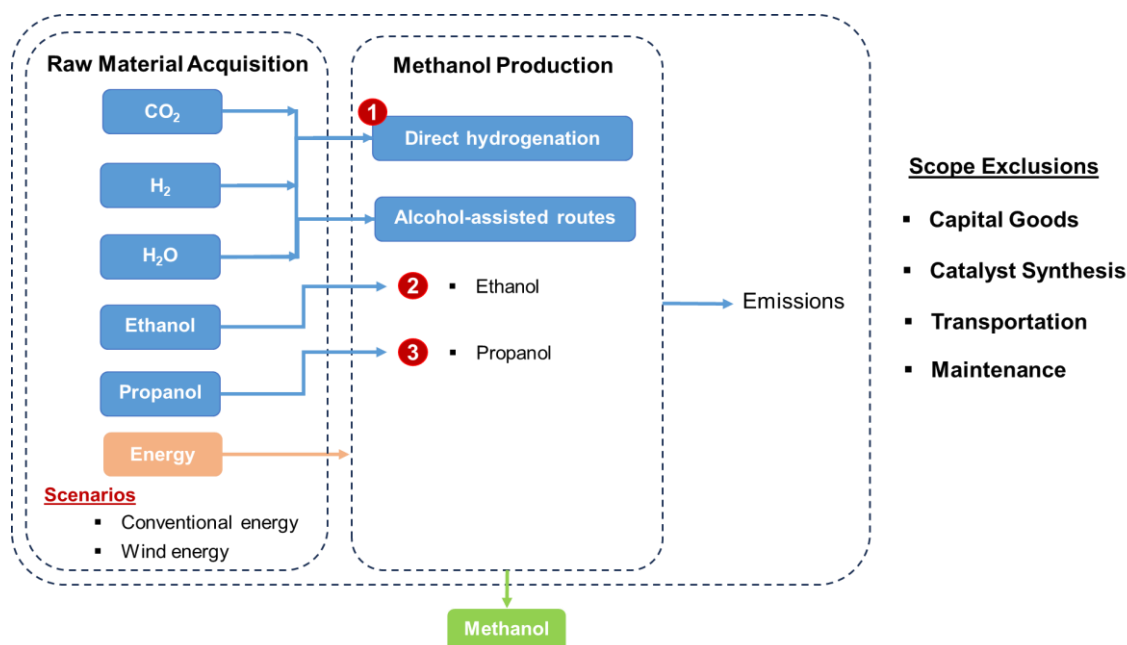


**Figure 4** System boundary and case scenarios of methanol production.

Two energy scenarios were considered: one using conventional heat from natural gas and electricity from the grid and the other using wind power for both heat and electricity. These scenarios were applied to all three methanol production routes: direct hydrogenation, ethanol-assisted, and propanol-assisted processes. The selection of wind energy in this study is consistent with Thailand's draft Power Development Plan (PDP) 2024, which targets an expansion of wind power capacity to 9,379 MW by 2037, mainly in the northeastern and southern regions, ranking second after solar energy (33,516 MW) (Department of Alternative Energy Development and Efficiency, 2022). Ongoing investments in Thailand include large-scale wind power projects totaling 286 MW and plans to expand installed capacity to 2,000 MW by 2037 (Bloomberg, 2025; GULF, 2025), demonstrating Thailand's growing commitment to wind power and its potential to meet future industrial demand. In terms of environmental impacts, wind energy offers several advantages over other renewable sources. Unlike solar power, which requires large land areas and relies on

minerals for photovoltaic panels, wind energy installations have a smaller land footprint and demand fewer mineral resources (Monirill) et al., 2022, Olabi et al., 2023). For these reasons, wind energy was selected to investigate the near-future feasibility of methanol production in this study.

The following components were excluded from the system boundaries: (1) capital goods; (2) catalyst synthesis; (3) transportation; and (4) maintenance. In this study, catalyst synthesis was excluded because the Cu/ZnO catalyst has a relatively long lifetime of approximately 2–6 years, depending on the operating conditions, and no inventory data are available for large-scale catalyst synthesis. Therefore, its contribution to the overall environmental impact per functional unit was considered negligible (Barrow et al., 2024). Transportation and maintenance were also excluded because their contributions were minimal compared with those of the main process stages. The data sources for the raw materials and utility acquisition are provided in Table 1.

**Table 1** Data sources for raw material and utility acquisition

| Raw materials and utilities | Data Source  |
|-----------------------------|--|
| Carbon dioxide              | Carbon dioxide, liquid {RoW}  market for carbon dioxide, liquid  |
| Hydrogen                    | Hydrogen, gaseous, low pressure {RoW}  hydrogen production, gaseous, petroleum refinery operation from natural gas                           |
| Cooling water               | Water, completely softened {RoW}  market for water, completely softened  |
| Ethanol                     | Ethanol, without water, in 99.7% solution state, from ethylene {RoW}  ethanol production, ethylene hydration                                 |
| Propanol                    | 1-propanol {RoW}  1-propanol production  |
| Conventional steam          | Heat, from steam, in chemical industry {RoW}  steam production, as energy carrier, in chemical industry                                      |
| Wind-powered steam          | Based on 1 MJ of steam production and a boiler efficiency of 90%, the system requires approximately 0.308 kWh of electricity from wind power |
| Grid electricity            | Electricity, medium voltage   electricity voltage transformation from high to medium voltage   |
| Wind-based electricity      | Electricity, high voltage {RoW}  electricity production, wind, >3MW turbine, onshore   |

To account for wind-powered steam generation, boiler efficiency was considered. Assuming a boiler efficiency of 90%, the energy input required to produce 1 MJ of steam was calculated by dividing the thermal energy output by the efficiency, yielding approximately 1.11 MJ. This value was converted to electricity demand via a conversion factor of 1 kWh = 3.6 MJ, resulting in an electricity requirement of approximately 0.308 kWh, on the basis of wind-generated electricity data. The construction, assembly, and infrastructure of wind turbines were excluded from the assessment, as their long operational lifespan renders the associated environmental impacts relatively negligible.

## Results and discussion

### 1) Inventory analysis

The results indicated that alcohol-assisted processes significantly reduced raw material consumption compared with the conventional route (Table 2). Specifically, the carbon dioxide input decreased by 14.79% and 10.29% when ethanol and propanol were used, respectively. For hydrogen, the reductions were 11.15% and 81.15% for the ethanol-assisted routes and propanol-assisted routes, respectively, compared with direct hydrogenation. The use of higher-molecular-weight alcohols such as ethanol and propanol in CO<sub>2</sub> hydrogenation can significantly reduce H<sub>2</sub> demand, as confirmed by inventory analysis. These alcohols participate in alternative reaction pathways involving C–C coupling and serve as hydrogen donors or intermediates, partially replacing the required H<sub>2</sub> and thereby lowering overall hydrogen consumption (Anbu and Dhakshinamoorthy, 2017; Joshi and Bollini, 2025). However, it is important to note that alcohol-assisted processes require ethanol and propanol as catalytic solvents, which are not used in the conventional route. Compared with the ethanol-assisted route, the propanol-assisted route requires approximately fifty-two times more alcohol by mass to achieve a 1:1 molar ratio of CO<sub>2</sub> to alcohol. The large difference in alcohol

make-up was due to the propanol process's low 26.57% single-pass methanol conversion, which was further reduced by a side reaction to form propyl propanoate, whereas ethanol reached 75.35% conversion without side reactions (Boonamnuai et al., 2021; Zeng et al., 2002). A similar alcohol make-up was reported in previous simulation studies (Mungchan, 2021).

In terms of utility consumption, the alcohol-assisted routes demand significantly more cooling water and steam than does the direct hydrogenation route because three distillation columns are used to separate methanol from gas, water, and alcohol. In contrast, the direct hydrogenation route involves a single distillation step. Among the three processes, the propanol-assisted route consumed the greatest amount of make-up cooling water and steam, followed by the ethanol-assisted route, whereas the direct hydrogenation route required the least. Air emissions show that alcohol-assisted routes are more environmentally favorable than conventional routes are, primarily because of lower CO<sub>2</sub> emissions. This improvement in environmental performance is attributed to the higher conversion efficiency facilitated by the catalyst, which enables more complete conversion of reactants to methanol and reduces the amount of unreacted gases, thereby lowering greenhouse gas emissions (Likhittaphon et al., 2019). In terms of water emissions, the alcohol-assisted routes significantly reduce methanol discharge compared with the conventional route but introduce ethanol and propanol emissions, which are absent in the conventional process. Notably, more waterborne pollutants are generated in the propanol-assisted route because of the dehydrogenative coupling of propanol to propyl propanoate (Anbu and Dhakshinamoorthy, 2017). In contrast, the ethanol-assisted route does not produce ethyl acetate via dehydrogenative coupling, likely because the catalyst activity favors methanol production through an alternative reaction pathway (Joshi and Bollini, 2025).

**Table 2** Inventory of methanol production

| List              | Item              | Unit | Direct hydrogenation | Alcohol-assisted route |           |
|-------------------|-------------------|------|----------------------|------------------------|-----------|
|                   |                   |      |                      | Ethanol                | Propanol  |
| Product           | Methanol          | kg   | 1,000.00             | 1,000.00               | 1,000.00  |
| Reactant          | Carbon dioxide    |      | 1,667.51             | 1,429.86               | 1,496.33  |
|                   | Hydrogen          |      | 217.72               | 193.45                 | 40.99     |
|                   | Ethanol           | kg   | -                    | 128.48                 | -         |
|                   | Propanol          |      | -                    | -                      | 6679.20   |
|                   | Cooling water     | kg   | 3,717.00             | 20,652.28              | 31,637.52 |
| Utilities         | Steam             | kWh  | 2,813.91             | 11,601.27              | 20,448.02 |
|                   | Electricity       | kWh  | 559.80               | 509.03                 | 695.40    |
|                   | Methanol          |      | 149.64               | 11.75                  | 22.10     |
| Emission to air   | Ethanol           |      | -                    | 3.79                   | -         |
|                   | Propanol          |      | -                    | -                      | -         |
|                   | Propyl propanoate | kg   | -                    | -                      | 5.66      |
|                   | Steam             |      | 26.85                | 0.10                   | 18.70     |
|                   | Hydrogen          |      | 0.74                 | 2.09                   | 0.04      |
|                   | Carbon dioxide    |      | 91.99                | 37.33                  | 83.53     |
|                   | Water             |      | 614.03               | 569.89                 | 573.16    |
|                   | Methanol          |      | 2.00                 | 2.12                   | 1.00      |
| Emission to water | Ethanol           | kg   | -                    | 124.82                 | -         |
|                   | Propanol          |      | -                    | -                      | 2,145.83  |
|                   | Propyl Propanoate |      | -                    | -                      | 4,366.50  |

## 2) Impact assessment and interpretation

The midpoint impacts revealed that the most significant impact categories were terrestrial ecotoxicity, global warming, human noncarcinogenic toxicity, and fossil resource scarcity (Table 3). Among the routes, the propanol-assisted process consistently presented the highest environmental burdens across all categories, with impacts significantly greater than those of the ethanol-assisted and direct hydrogenation routes. The ethanol-assisted route had moderate environmental impacts, whereas the direct hydrogenation route had the lowest overall impact.

The normalized results shown in Figure 5 were analyzed to assess the contributions of individual inventory components to the overall environmental impacts of the methanol production process, aiming to identify specific impact hotspots.

In the direct hydrogenation route, the acquisition of liquefied CO<sub>2</sub> is a major contributor to environmental impacts because of its high energy demand and reliance on fossil fuels. The energy-intensive liquefaction process has led to substantial greenhouse gas emissions, contributing to global warming, ozone depletion, and mineral resource scarcity (Tamura et al., 2001). The land use impacts were associated with fossil fuel extraction and infrastructure development. Additionally, emissions from fossil fuel-based energy production contribute to water ecotoxicity and eutrophication via the release of nitrogen oxides, sulfur oxides, and heavy metals (Al-Shayji and Aleisa, 2018; Gaete-Morale et al., 2019; Wahyono et al., 2022). Therefore, liquefied CO<sub>2</sub> acquisition was identified as a key environmental hotspot in this pathway. Steam acquisition is another significant contributor, owing to

its high energy requirement and use of carbon-intensive fuels. Steam was essential for maintaining the reaction temperature and supporting the separation processes. Its production via fossil fuel combustion has resulted in emissions that contribute to global warming, particulate matter formation, ozone depletion, and water ecotoxicity (Bach, 1981; Inumaru et al., 2021).

Electricity acquisition from the Thai grid also impacts categories such as freshwater eutrophication, water ecotoxicity, and human health. This was due to the grid's continued reliance on fossil fuels, including coal and natural gas, leading to emissions of nitrogen oxides (NO<sub>x</sub>), sulfur dioxide (SO<sub>2</sub>), and heavy metals (Chhay and Limmeechokchai, 2019; Misila et al., 2020). The acquisition of hydrogen from petroleum refinery operations has contributed significantly to fossil and mineral resource scarcity because of substantial natural gas consumption (Wang and Azam, 2024). Additionally, methanol emissions to the atmosphere contributed to ozone formation in both the human health and terrestrial ecosystem impact categories. As a volatile organic compound (VOC), methanol reacts with sunlight to form ground-level ozone, which poses risks to respiratory health and vegetation (Cheng et al., 2021; Luo et al., 2020).

In the ethanol-assisted route, the primary environmental contributors shifted from CO<sub>2</sub> and H<sub>2</sub> to steam and ethanol due to the additional distillation steps required for ethanol separation and recycling. These steps increased the steam demand and make-up cooling water consumption, increasing the overall energy intensity. Ethanol acquisition via ethylene hydration had relatively low impacts in most categories owing to the high conversion efficiency and low emissions associated with the process

(Global LCA Data Access, 2011). In the propanol-assisted route, propanol acquisition was the dominant contributor across all impact categories. This was due to both the significantly greater quantity required and the energy-intensive recovery process associated with the higher boiling point of propanol. Additionally, typical production via fossil-based hydroformylation of propylene further intensified upstream emissions and resource use (Liu et al., 2020). The complex separation processes and increased steam and cooling water requirements further

increase CO<sub>2</sub> emissions and resource consumption, especially in energy-intensive recovery stages (Mungchan, 2021). The higher energy demand for propanol separation arose mainly from the larger mass flow of propanol entering the distillation column. Although ethanol–water separation is generally energy intensive, the greater alcohol feed in the propanol-assisted route increased the vaporization load, resulting in greater reboiler duty and overall energy consumption.

**Table 3** Midpoint impacts per functional unit using conventional energy sources

| Impact category                         | Unit                     | Direct hydrogenation  | Alcohol-assisted route |                       |
|---|--------------------------|-----------------------|------------------------|-----------------------|
|   |                          |                       | Ethanol                | Propanol              |
| Global warming                          | kg CO <sub>2</sub> eq    | 3.87                  | 7.74                   | 52.90                 |
| Stratospheric ozone depletion           | kg CFC11 eq              | 6.11×10 <sup>-7</sup> | 1.01×10 <sup>-6</sup>  | 9.41×10 <sup>-6</sup> |
| Ionizing radiation                      | kBq Co-60 eq             | 5.85×10 <sup>-2</sup> | 8.07×10 <sup>-2</sup>  | 1.57                  |
| Ozone formation, human health           | kg NO <sub>x</sub> eq    | 1.25×10 <sup>-2</sup> | 1.19×10 <sup>-2</sup>  | 0.14                  |
| Fine particulate matter formation       | kg PM2.5 eq              | 3.50×10 <sup>-3</sup> | 6.86×10 <sup>-3</sup>  | 6.87×10 <sup>-2</sup> |
| Ozone formation, terrestrial ecosystems | kg NO <sub>x</sub> eq    | 1.74×10 <sup>-2</sup> | 1.36×10 <sup>-2</sup>  | 0.17                  |
| Terrestrial acidification               | kg SO <sub>2</sub> eq    | 8.27×10 <sup>-3</sup> | 1.73×10 <sup>-2</sup>  | 0.14                  |
| Freshwater eutrophication               | kg P eq                  | 8.76×10 <sup>-4</sup> | 1.48×10 <sup>-3</sup>  | 1.69×10 <sup>-2</sup> |
| Marine eutrophication                   | kg N eq                  | 1.31×10 <sup>-4</sup> | 1.65×10 <sup>-4</sup>  | 1.09×10 <sup>-3</sup> |
| Terrestrial ecotoxicity                 | kg 1,4-DCB               | 13.93                 | 26.56                  | 111.11                |
| Freshwater ecotoxicity                  | kg 1,4-DCB               | 2.50×10 <sup>-2</sup> | 4.17×10 <sup>-2</sup>  | 0.47                  |
| Marine ecotoxicity                      | kg 1,4-DCB               | 3.80×10 <sup>-2</sup> | 6.70×10 <sup>-2</sup>  | 0.70                  |
| Human carcinogenic toxicity             | kg 1,4-DCB               | 0.10                  | 0.18                   | 2.25                  |
| Human noncarcinogenic toxicity          | kg 1,4-DCB               | 1.27                  | 2.21                   | 24.67                 |
| Land use                                | m <sup>2</sup> a crop eq | 1.74×10 <sup>-2</sup> | 2.85×10 <sup>-2</sup>  | 0.73                  |
| Mineral resource scarcity               | kg Cu eq                 | 2.14×10 <sup>-4</sup> | 3.92×10 <sup>-4</sup>  | 5.34×10 <sup>-3</sup> |
| Fossil resource scarcity                | kg oil eq                | 1.48                  | 2.67                   | 19.21                 |
| Water consumption                       | m <sup>3</sup>           | 1.20×10 <sup>-2</sup> | 3.16×10 <sup>-2</sup>  | 0.63                  |

The global warming potential (GWP) was assessed across three key sectors of methanol production: raw material sourcing, energy consumption (compression, reaction, and separation stages), and emissions (Figure 6). Among these factors, raw material acquisition had the strongest influence on GWP, particularly due to the inclusion of alcohols. The high energy intensity of alcohol production directly contributed to the GWP, representing a trade-off in the alcohol-assisted routes, where the use of alcohols reduced the consumption of primary reactants such as CO<sub>2</sub> and H<sub>2</sub>. In the direct hydrogenation route, the GWP from CO<sub>2</sub> and H<sub>2</sub> acquisition was 2.062 kg CO<sub>2</sub>-eq. This value was reduced to 1.786 kg CO<sub>2</sub>-eq (13.39%) in the ethanol-assisted route and to 1.455 kg CO<sub>2</sub>-eq (29.45%) in the propanol-assisted route. As discussed earlier, this reduction was due to the alcohols acting as hydrogen donors via dehydrogenative esterification reactions, thereby lowering the external hydrogen demand (Anbu and Dhakshinamoorthy, 2017; Joshi and Bollini, 2025). However, the large quantity of propanol required in Case 3 offset part of this benefit through increased upstream emissions.

With respect to the GWP from the energy sector, the alcohol-assisted routes showed improved performance in both the compression and reaction stages relative to the direct hydrogenation route. Specifically, the compression-related GWP decreased by 13.15% (0.363 kg CO<sub>2</sub>-eq) in the ethanol-assisted route and by 64.11% (0.150 kg CO<sub>2</sub>-eq) in the propanol-assisted route compared with 0.418 kg CO<sub>2</sub>-eq in the direct hydrogenation route. This improvement was attributed to lower input flows of CO<sub>2</sub> and H<sub>2</sub>, which reduced the compression energy demand. Additionally, a small GWP contribution originated from the pump used to introduce liquid alcohol: 0.011 kg CO<sub>2</sub>-eq in the ethanol-assisted route and 0.055 kg CO<sub>2</sub>-eq in the propanol-assisted route. Furthermore, the alcohol-assisted routes operated at a substantially lower reaction temperature (150 °C) than 250 °C in the direct hydrogenation process. This temperature reduction significantly decreased the energy demand from lower heat requirements in the preheating and reactor sections, leading to an approximately 98.68% reduction in the reaction-stage GWP—from 0.836 kg CO<sub>2</sub>-eq to 0.011 kg CO<sub>2</sub>-eq in both alcohol-assisted cases. The lower thermal requirements contributed to overall energy savings and further mitigated climate-related impacts.



**Figure 5** Normalized results for methanol production: (a) direct hydrogenation route, (b) ethanol-assisted route, and (c) propanol-assisted route.

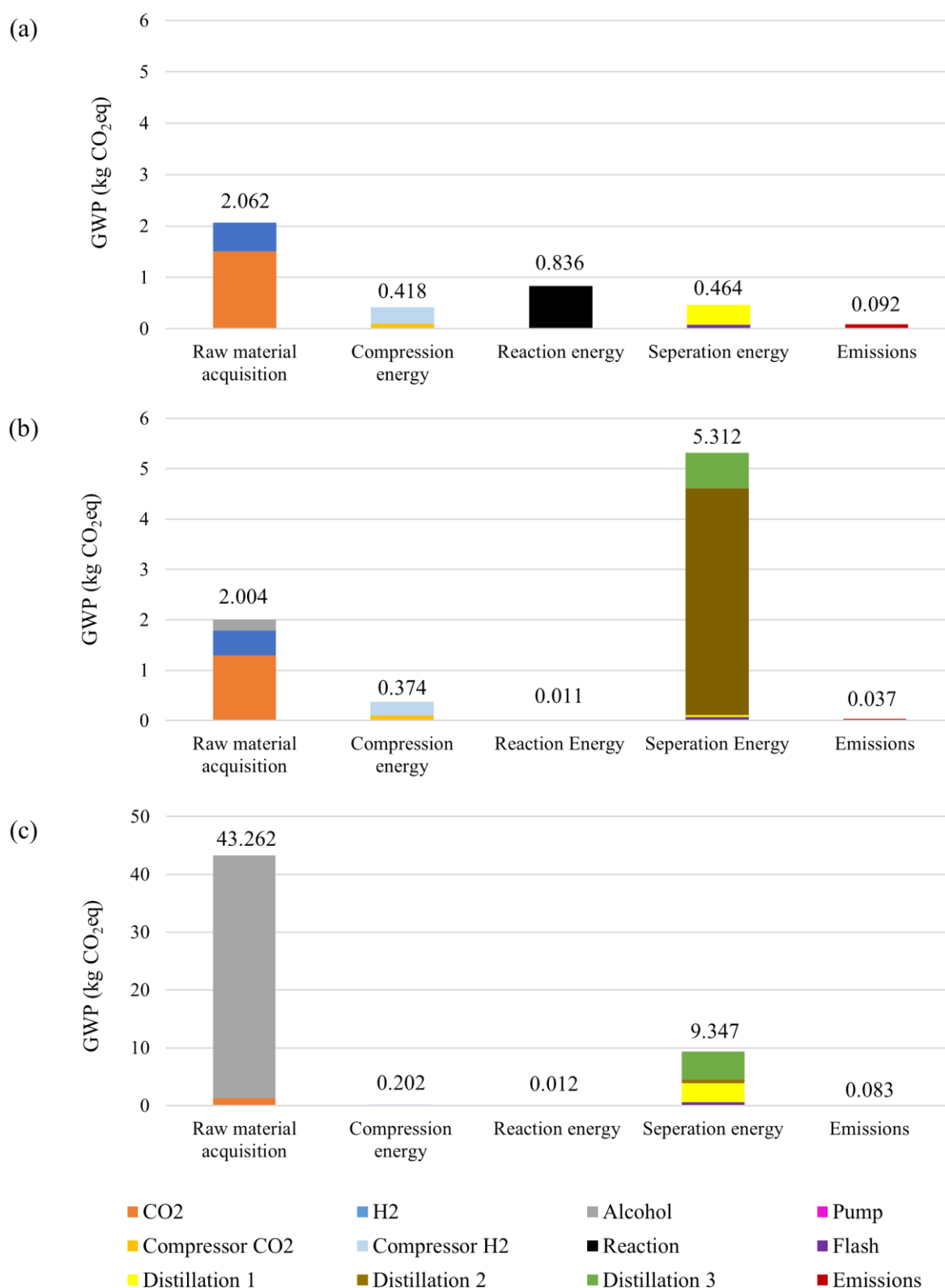


**Figure 6** Global warming potential by section of methanol production: (a) direct hydrogenation route, (b) ethanol-assisted route, and (c) propanol-assisted route.

However, the energy-related GWP in the separation stage was greater in the alcohol-assisted routes because of the additional distillation requirements for product separation and alcohol recovery. The total GWP from the distillation and flash units was 0.464 kg CO<sub>2</sub>-eq in the direct hydrogenation route, whereas it was 5.312 kg CO<sub>2</sub>-eq in the ethanol-assisted route and 9.347 kg

CO<sub>2</sub>-eq in the propanol-assisted route. In the ethanol-assisted process, the primary hotspot was the second distillation column used to separate methanol and ethanol from water. The azeotropic nature of the ethanol–water mixture made this separation highly energy intensive (Kanse and Dawande, 2017; Peng et al., 2017). Similarly, in the propanol-assisted route, the main hotspot was

the third distillation column, which separates propanol and propyl propanoate for solvent recycling. The close-boiling nature of these compounds results in high steam and cooling requirements, further increasing energy consumption and GWP (Devale and Mahajan, 2024; Yang et al., 2024).

To mitigate the environmental impacts of alcohol-assisted routes, steam generation was identified as a major hotspot across all impact categories in all three scenarios. Accordingly, the steam source in the life cycle

inventory was replaced with wind-powered electricity. In addition, process electricity was substituted with wind-derived power. Table 4 presents the resulting midpoint impact indicators for the three scenarios, which use steam and electricity sourced from wind energy, along with the percentage changes relative to the conventional energy cases. The normalized environmental impacts for each methanol production route using wind-powered energy are shown in Figure 7.



**Figure 7** Normalized impacts of methanol production via wind-powered energy: (a) direct hydrogenation, (b) ethanol-assisted route, and (c) propanol-assisted route.

**Table 4** Midpoint impacts per functional unit using wind-powered steam and electricity

| Impact category                         | Unit                     | Direct hydrogenation<br>(Wind power) | %<br>Change | Alcohol-assisted<br>route: Ethanol<br>(Wind power) | %<br>Change | Alcohol-assisted<br>route: Propanol<br>(Wind power) | %<br>Change |
|---|--------------------------|--------------------------------------|-------------|--|-------------|---|-------------|
| Global warming                          | kg CO <sub>2</sub> eq    | 2.18                                 | -44.61%     | 2.10   | -73.65%     | 43.43   | -18.71%     |
| Stratospheric ozone depletion           | kg CFC11 eq              | 3.61×10 <sup>-7</sup>                | -40.86%     | 3.49×10 <sup>-7</sup>                              | -65.42%     | 8.28×10 <sup>-6</sup>                               | -11.95%     |
| Ionizing radiation                      | kBq Co-60 eq             | 4.99×10 <sup>-2</sup>                | -14.64%     | 4.68×10 <sup>-2</sup>                              | -42.04%     | 1.52  | -3.79%      |
| Ozone formation, human health           | kg NO <sub>x</sub> eq    | 1.01×10 <sup>-2</sup>                | -19.00%     | 4.17×10 <sup>-3</sup>                              | -64.93%     | 0.13  | -9.50%      |
| Fine particulate matter formation       | kg PM2.5 eq              | 2.03×10 <sup>-3</sup>                | -42.05%     | 1.97×10 <sup>-3</sup>                              | -71.26%     | 6.02×10 <sup>-2</sup>                               | -12.34%     |
| Ozone formation, terrestrial ecosystems | kg NO <sub>x</sub> eq    | 1.49×10 <sup>-2</sup>                | -14.55%     | 5.27×10 <sup>-3</sup>                              | -61.17%     | 0.16  | -8.27%      |
| Terrestrial acidification               | kg SO <sub>2</sub> eq    | 4.36×10 <sup>-3</sup>                | -47.28%     | 4.26×10 <sup>-3</sup>                              | -75.41%     | 0.12  | -15.77%     |
| Freshwater eutrophication               | kg P eq                  | 3.58×10 <sup>-4</sup>                | -59.10%     | 4.01×10 <sup>-4</sup>                              | -72.89%     | 1.51×10 <sup>-2</sup>                               | -10.58%     |
| Marine eutrophication                   | kg N eq                  | 8.97×10 <sup>-5</sup>                | -31.34%     | 8.19×10 <sup>-5</sup>                              | -50.44%     | 9.50×10 <sup>-4</sup>                               | -12.64%     |
| Terrestrial ecotoxicity                 | kg 1,4-DCB               | 9.46                                 | -32.04%     | 8.62   | -67.56%     | 79.53   | -28.42%     |
| Freshwater ecotoxicity                  | kg 1,4-DCB               | 1.12×10 <sup>-2</sup>                | -55.20%     | 1.19×10 <sup>-2</sup>                              | -71.53%     | 0.42  | -10.48%     |
| Marine ecotoxicity                      | kg 1,4-DCB               | 1.66×10 <sup>-2</sup>                | -56.40%     | 1.67×10 <sup>-2</sup>                              | -75.08%     | 0.62  | -12.01%     |
| Human carcinogenic toxicity             | kg 1,4-DCB               | 5.08×10 <sup>-2</sup>                | -49.89%     | 5.19×10 <sup>-2</sup>                              | -71.61%     | 2.03  | -9.87%      |
| Human noncarcinogenic toxicity          | kg 1,4-DCB               | 0.57                                 | -54.64%     | 0.55   | -74.97%     | 21.88   | -11.31%     |
| Land use                                | m <sup>2</sup> a crop eq | 1.25×10 <sup>-2</sup>                | -28.36%     | 1.28×10 <sup>-2</sup>                              | -55.27%     | 0.71  | -3.72%      |
| Mineral resource scarcity               | kg Cu eq                 | 1.48×10 <sup>-4</sup>                | -30.89%     | 1.71×10 <sup>-4</sup>                              | -56.37%     | 4.96×10 <sup>-3</sup>                               | -7.18%      |
| Fossil resource scarcity                | kg oil eq                | 0.97                                 | -34.36%     | 1.00   | -62.78%     | 16.30   | -15.16%     |
| Water consumption                       | m <sup>3</sup>           | 9.68×10 <sup>-3</sup>                | -19.45%     | 2.67×10 <sup>-2</sup>                              | -15.57%     | 0.62  | -1.30%      |

A substantial reduction in the global warming potential was observed in the ethanol-assisted case, which can be further explained through a sectional analysis of the production process (Figure 8). This analysis revealed that the use of wind energy significantly reduced the global warming potential across the compression, reaction, and separation stages for all three production routes. However, even when the global warming potential from energy use, emissions, and raw material acquisition is combined, the ethanol-assisted route still has the lowest overall impact. As previously discussed in the inventory analysis, this improvement is attributed primarily to the higher CO<sub>2</sub> conversion efficiency achieved via this route, which led to lower CO<sub>2</sub> emissions—a dominant contributor to the global warming potential. Additionally, the reduced consumption of CO<sub>2</sub>, H<sub>2</sub>, and ethanol further contributed to the improved environmental performance of the ethanol-assisted route compared with that of direct hydrogenation.

These findings demonstrate the enhanced sustainability of methanol production via the ethanol-assisted route when powered by wind energy. From the validation of the LCA results, in the case of CO<sub>2</sub> direct hydrogenation, the GWP obtained in this work was 3.87 kg CO<sub>2</sub>-eq/kg methanol, which aligned with reported values of approximately 2.2–4.3 kg CO<sub>2</sub>-eq/kg methanol for the same Cu/ZnO catalyst under similar operating conditions. The variation depended on the electricity source used—2.2 kg CO<sub>2</sub>-eq/kg methanol for natural gas combined cycle (NGCC)-based electricity and 4.3 kg CO<sub>2</sub>-eq/kg methanol for coal-based electricity (Artz et al., 2018). Furthermore, the primary hotspot contribution from heat demand observed in this study was consistent with previous findings. In contrast, earlier gate-to-gate alcohol-assisted methanol production studies with narrower system boundaries did not report overall CO<sub>2</sub> emissions, which were approximately 20,000 ton CO<sub>2</sub> per year for the ethanol route, with energy use identified as the primary impact contributor (Mungchan, 2021). Similarly, steam was a major contributor to the cradle-to-gate analysis. This comparison underscores the importance of integrating upstream processes in LCA studies and suggests that sourcing raw materials from low-impact or renewable processes could substantially improve environmental performance in future work.

## Conclusions

This study conducted a life cycle assessment of methanol production via direct CO<sub>2</sub> hydrogenation, ethanol-assisted, and propanol-assisted routes, demonstrating that alcohol-assisted processes—particularly the ethanol-assisted route—can provide environmental and process advantages under specific conditions. Under the conventional energy scenario, the direct CO<sub>2</sub> hydrogenation route presented the lowest environmental

impacts across most categories, including the global warming potential. Although the alcohol-assisted routes operated at lower reaction temperatures and required less CO<sub>2</sub> and H<sub>2</sub>, they incurred significantly higher energy consumption during separation and purification. This issue was most severe in the propanol-assisted route, which presented the highest global warming potential and overall environmental burdens due to greater alcohol feedstock requirements, increased utility consumption, and the energy-intensive nature of distillation and solvent recovery. While the ethanol-assisted route performed better than the propanol-assisted route did, its global warming potential remained higher than that of direct hydrogenation, primarily because of the energy required for alcohol recycling and methanol purification.

When wind energy was substituted for conventional heat and electricity, all three methanol production routes exhibited substantial reductions in global warming potential. The most notable improvement occurred in the ethanol-assisted route, where renewable electricity significantly reduced the environmental burden of the separation stage. In this scenario, the ethanol-assisted route became the most environmentally favorable, achieving the lowest global warming potential among all cases. Although the propanol-assisted route also benefits from wind energy, its overall impact remains relatively high because of inherently greater material and energy demands.

Future research should focus on improving the efficiency of alcohol recovery and methanol purification, integrating renewable energy sources, and evaluating the use of biobased or recycled alcohols. In addition, emphasis should be placed on the sustainable sourcing of H<sub>2</sub> and CO<sub>2</sub>, which should be supported by techno-economic analysis and pilot-scale validation to ensure industrial applicability and environmental sustainability.

## Acknowledgements

The authors would like to express their deep gratitude to the Malaysia-Thailand Joint Authority (MTJA) for funding that made this research possible, as well as to the Faculty of Engineering at Kasetsart University for providing additional resources, institutional support, and funding throughout the project (Grant No. 67/01/CHEM/D.Eng).

## Data availability statement

Information and data used in the study will be disclosed upon request.

## Author ORCID

**Chayet Worathitanon:** 0009-0005-4091-0628

**Kritsana Suwanamad:** 0009-0008-5342-4778

**Viganda Varabuntoonvit:** 0000-0003-0641-3052

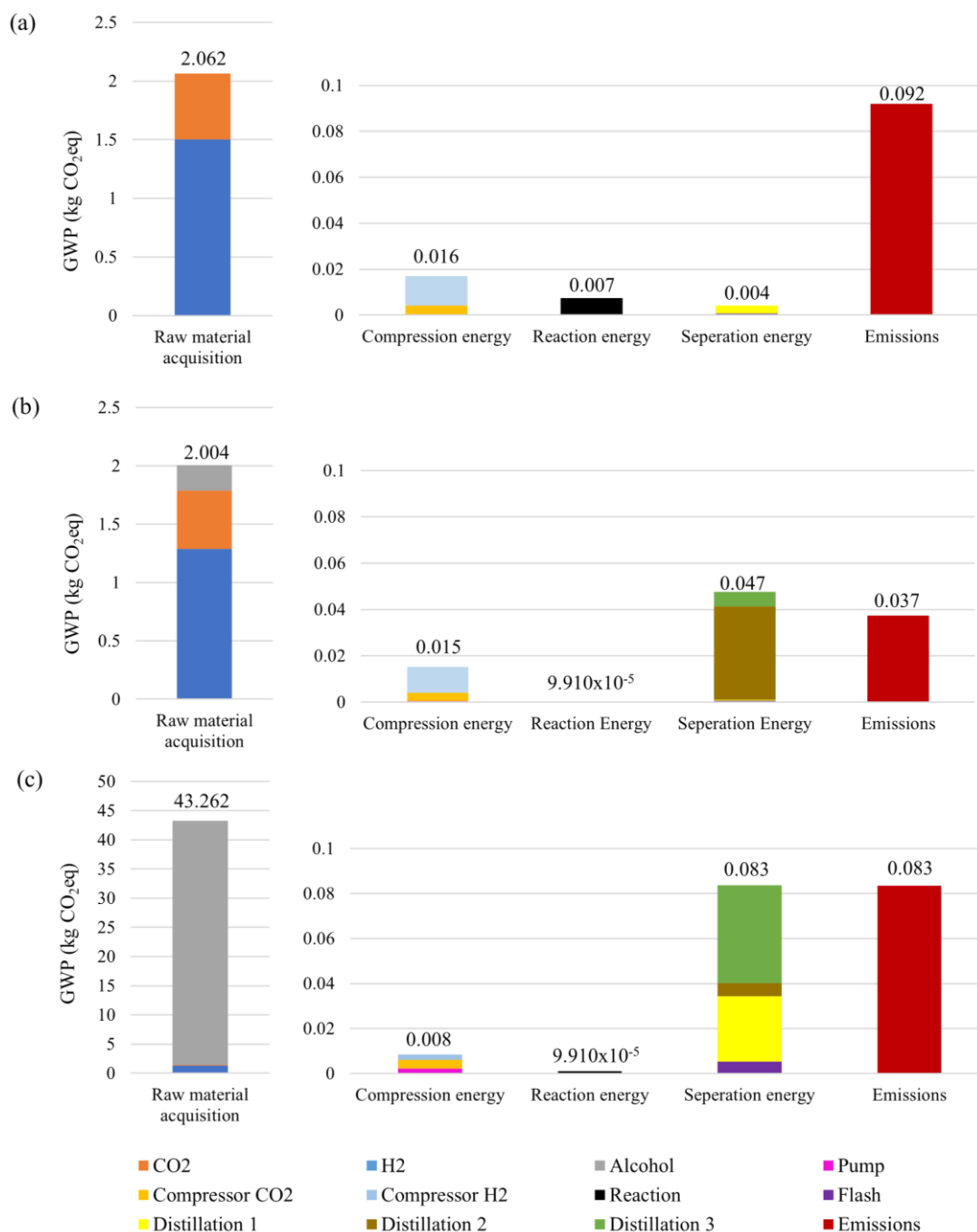


**Figure 8** Global warming potential by section of methanol production using wind-powered energy: (a) Direct hydrogenation, (b) ethanol-assisted route, and (c) propanol-assisted route.

**Author contributions**

**Chayet Worathitanon:** Software, Validation, Formal analysis, Investigation, Data curation, Writing – Original draft, Writing – Review & editing, Visualization, Project administration

**Naphat Chansonthi:** Software, Formal analysis, Writing – Original draft

**Pawat Pinthong:** Software, Formal analysis, Writing – Original draft

**Kritsana Suwanamad:** Software, Validation

**Viganda Varabuntoonvit:** Conceptualization, Methodology, Validation, Formal analysis, Investigation, Resources, Writing – Review & editing, Visualization, Supervision, Funding acquisition

**Conflicts of interest**

The authors declare that there are no conflicts of interest in competing financial or personal relationships that could have appeared to influence the work reported in this work.

**References**

Ahmed, O. Y., Ries, M. J., & Northrop, W. F. (2019). Emissions factors from distributed, small-scale biomass gasification power generation: Comparison to open burning and large-scale biomass power generation. *Atmospheric Environment*, 200, 221–227.

Al-Shayji, K., & Aleisa, E. (2018). Characterizing the fossil fuel impacts in water desalination plants in

- Kuwait: A Life Cycle Assessment approach. *Energy*, 158, 681–692.
- Anbu, N., & Dhakshinamoorthy, A. (2017). Cu<sub>3</sub>(BTC)<sub>2</sub> catalyzed dehydrogenative coupling of dimethylphenylsilane with phenol and homocoupling of dimethylphenylsilane to disiloxane. *Journal of Colloid and Interface Science*, 490, 430–435.
- Artz, J., Muller, T., Thenert, K., Kleinekorte, J., Meys, R., Sternberg, A., Bardow, A., & Leitner W. (2018). Sustainable conversion of carbon dioxide: An integrated review of catalysis and life cycle assessment. *Chemical Reviews*, 118(2), 434–504.
- Barrow, N., Bradley, J., Corrie, B., Cui, Y., Tran, T.D., Erden, T.E., Fish, A., Garcia, M., Glen, P., Mistry, N., Nicholson, M., Roloff-Standing, S., Shelton, D., Smith, T., Summer, A., Din, K. U., & Macleod N. (2024). Doubling the life of Cu/ZnO methanol synthesis catalysts via use of Si as a structural promoter to inhibit sintering. *Science Advances*, 10(3), 10793955.
- Bach, W. (1981). Fossil fuel resources and their impacts on environment and climate. *International Journal of Hydrogen Energy*, 6(2), 185–201.
- Bloomberg. (2025). *Top Thai wind power firm to fund \$2 billion spending by IPO*. Retrieved October 18, 2025, from <https://www.bloomberg.com/news/articles/2025-05-29/top-thai-wind-power-firm-to-fund-2-billion-of-spending-with-ipo?embedded-checkout=true>
- Bolan, S., Padhye, L. P., Jasemizad, T., Govarthan, M., Karmegam, N., Wijesekara, H., Amarasiri, D., Hou, D., Zhou, P., Biswal, B. K., Balasubramanian, R., Wang, H., Siddique, K. H. M., Rinklebe, J., Kirkham, M. B., & Bolan, N. (2024). Impacts of climate change on the fate of contaminants through extreme weather events. *Science of the Total Environment*, 909, 168388.
- Boonamnuai, T., Laosiripojana, N., Assabumrungrat, S., & Kim-Lohsoontorn, P. (2021). Effect 3A and 5A molecular sieve on alcohol-assisted methanol synthesis from CO<sub>2</sub> and H<sub>2</sub> over Cu/ZnO catalyst. *International Journal of Hydrogen Energy*, 46(60), 30948–3095.
- Cheng, N., Jing, D., Zhang, C., Chen, Z., Li, W., Li, S., & Wang Q. (2021). Process-based VOCs source profiles and contributions to ozone formation and carcinogenic risk in a typical chemical synthesis pharmaceutical industry in China. *Science of the Total Environment*, 752, 141899.
- Chhay, L., & Limmeechokchai, B. (2019). CO<sub>2</sub> mitigation in the power sector of Thailand: Analyses of cleaner supply-side options beyond the Paris Agreement. *The Open Environmental Research Journal*, 12, 15–25.
- Department of Alternative Energy Development and Efficiency (DEDE), Ministry of Energy. (2022). *Draft Alternative Energy Development Plan (AEDP) 2022–2037*. Department of Alternative Energy Development and Efficiency. <https://old.energy.go.th/wp-content/uploads/2022/09/04-%E0%B8%87%E0%B8%8B-AEDP-2022210965-Final.pdf>
- Devale, R. R., & Mahajan, Y. S. (2024). Separation of N-propyl propionate from its highly non-ideal reaction mixture: Distillation using rigorous simulation. *Materials Today: Proceedings*, 102, 410–415.
- Dinca, C., Slavu, N., Cormoș, C. C., & Badea, A. (2018). CO<sub>2</sub> capture from syngas generated by a biomass gasification power plant with chemical absorption process. *Energy*, 149, 925–936
- Gaete-Morales, C., Gallego-Schmid, A., Stamford, L., & Azapagic, A. (2019). Life cycle environmental impacts of electricity from fossil fuels in Chile over a ten-year period. *Journal of Cleaner Production*, 232, 1499–1512.
- Global LCA Data Access. (2011). *Global LCA data access*. Retrieved June 1, 2025, from <https://www.globallcadataaccess.org/ethylene-hydration-upr-ecoinvent-36-allocation-cut-1>
- GULF. (2025). *GULF joins forces with Goldwind to advance clean energy with turbine supply agreement for four wind farms in Thailand*. Retrieved October 18, 2025, from <https://www.gulf.co.th/en/newsroom/news-and-activities/502/gulf-joins-forces-with-goldwind-to-advance-clean-energy-with-turbine-supply-agreement-for-four-wind-farms-in-thailand>
- International Energy Agency. (2025). *Global Energy Review 2025*. International Energy Agency. <https://www.iea.org/reports/global-energy-review-2025>
- Inumaru, J., Hasegawa, T., Shirai, H., Nishida, H., Noda, N., & Ohyama, S. (2021). 1 - Fossil fuels combustion and environmental issues. In Ozawa, M., Asano, H. (Eds.), *Advances in power boilers* (pp. 1–56). Elsevier.
- El Farsaoui, M., Uratani, J. M., Zahra, M. A., & Griffiths, S. (2025). Establishing leadership in bringing carbon capture, utilisation and storage to scale. *Energy Research & Social Science*, 121, 103960.
- Esfahani, H. S., Khoshsima, A., Pazuki, G., & Hosseini, A. (2023). Separation of methanol and ethanol from azeotropic MTBE mixtures using choline chloride-based deep eutectic solvents. *Journal of Molecular Liquids*, 381, 121641.
- Joshi, V. V., & Bollini, P. (2025). Exploiting proximity effects to improve ethyl acetate selectivity in the dehydrogenative coupling of ethanol over supported Cu catalysts. *Applied Catalysis A: General*, 697, 120228.
- Kanse, N. G., & Dawande, S. D. (2017). Separation of ethanol/water (azeotropic mixture) by pervaporation using PVA membrane. *Materials Today: Proceedings*, 4(9), 10520–10523.
- Kim, C., Yoo, C. J., Oh, H. S., Min, B.K., & Lee, U. (2022). Review of carbon dioxide utilization technologies and their potential for industrial application. *Journal of CO<sub>2</sub> Utilization*, 65, 102239.
- Likhittaphon, S., Panyadee, R., Fakyam, W., Charojrochkul, S., Sornchamni, T., Laosiripojana, N., Assabumrungrat, S., & Kim-Lohsoontorn, P. (2019). Effect of CuO/ZnO

- catalyst preparation condition on alcohol-assisted methanol synthesis from carbon dioxide and hydrogen. *International Journal of Hydrogen Energy*, 44(37), 20782–20791.
- Liu, D., Chaudhari, R.V., & Subramaniam, B. (2020). Enriching propane/propylene mixture by selective propylene hydroformylation: Economic and environmental impact analyses. *ACS Sustainable Chemistry & Engineering*, 8(13), 5140–5146.
- Luo, H., Li, G., Chen, J., Lin, Q., Ma, S., Wang, Y., & An T. (2020). Spatial and temporal distribution characteristics and ozone formation potentials of volatile organic compounds from three typical functional areas in China. *Environmental Research*, 183, 109141.
- Misila, P., Winyuchakrit, P., & Limmeechokchai, B. (2020). Thailand's long-term GHG emission reduction in 2050: The achievement of renewable energy and energy efficiency beyond the NDC. *Heliyon*, 6(12), e05720.
- Mohamed, U., Zhao, Y. J., Yi, Q., Shi, L. J., Wei, G. Q., & Nimmo, W. (2021). Evaluation of life cycle energy, economy and CO<sub>2</sub> emissions for biomass chemical looping gasification to power generation. *Renewable Energy*, 176, 366–387.
- Moniril Islam, M., Sohag, K., Hammoudeh, S., Mariev, O., & Samargandi, N. (2022). Minerals import demands and clean energy transitions: A disaggregated analysis. *Energy Economics*, 113, 106205.
- Mungchan, P. (2021). Techno-economic analysis of alcohol-assisted methanol synthesis process: Effect of alcohol type and operating temperature. [Master Thesis, Chulalongkorn University].
- Olabi, A. G., Elsaid, K., Obaideen, K., Abdelkareem, M. A., Rezk, H., Wilberforce, T., Maghrabie, H. M., & Sayed E. T. (2023). Renewable energy systems: Comparisons, challenges and barriers, sustainability indicators, and the contribution to UN sustainable development goals. *International Journal of Thermofluids*, 20, 100498.
- Peng, Y., Lu, X., Liu, B., & Zhu, J. (2017). Separation of azeotropic mixtures (ethanol and water) enhanced by deep eutectic solvents. *Fluid Phase Equilibria*, 448, 128–134.
- Saidur, R., Rahim, N. A., Islam, M. R., & Solangi, K. H. (2011). Environmental impact of wind energy. *Renewable and Sustainable Energy Reviews*, 15(5), 2423–2430.
- Schumacher, L. (2016). ReCiPe. Retrieved October 18, 2025, from <https://pre-sustainability.com/articles/recipe/>
- Tamura, I., Tanaka, T., Kagajo, T., Kuwabara, S., Yoshioka, T., Nagata, T., Kurahashi, K., & Ishitani H. (2001). Life cycle CO<sub>2</sub> analysis of LNG and city gas. *Applied Energy*, 68(3), 301–319.
- Van-Dal, É. S., & Bouallou, C. (2013). Design and simulation of a methanol production plant from CO<sub>2</sub> hydrogenation. *Journal of Cleaner Production*, 57, 38–45.
- Wahyono, Y., Hadiyanto, H., Gheewala, S. H., Budihardjo, M. A., & Adiansyah, J. S. (2022). Evaluating the environmental impacts of the multi-feedstock biodiesel production process in Indonesia using life cycle assessment (LCA). *Energy Conversion and Management*, 266, 115832.
- Wang, J., & Azam, W. (2024). Natural resource scarcity, fossil fuel energy consumption, and total greenhouse gas emissions in top emitting countries. *Geoscience Frontiers*, 15(2), 101757.
- Xu, K., Chang, J., Zhou, W., Li, S., Shi, Z., Zhu, H., Chen, Y., & Guo K. (2022). A comprehensive estimate of life cycle greenhouse gas emissions from onshore wind energy in China. *Journal of Cleaner Production*, 338, 130683.
- Yang, F., Wu, T., Song, T., Zhang, Q., & Zhang, Z. (2024). Separation of n-propanol - n-propyl acetate azeotropic system by extractive distillation with ionic liquids: COSMO-RS prediction, experimental investigation and quantum chemical calculation. *Journal of Molecular Liquids*, 396, 124007.
- Ye, L., Xiao, P., Scales, P., Webley, P., Singh, R., & Li, G. K. (2023). Improved copper-based catalysts for alcohol-assisted CO<sub>2</sub> hydrogenation: A comparative study between novel nano-stabilized and deposition-precipitation method. *Molecular Catalysis*, 547, 113289.
- Yusuf, N., & Almomani, F. (2023). Highly effective hydrogenation of CO<sub>2</sub> to methanol over Cu/ZnO/Al<sub>2</sub>O<sub>3</sub> catalyst: A process economy & environmental aspects. *Fuel*, 332, 126027.
- Zeng, J. Q., Tsubaki, N., & Fujimoto, K. (2002). The promoting effect of alcohols in a new process of low-temperature synthesis of methanol from CO/CO<sub>2</sub>/H<sub>2</sub>. *Fuel*, 81(1), 125–127.